in the experiments described above.

The ability to photogenerate the reactive intermediate *trans*-$[PtH_2(PEt_3)_2]$ from the binuclear complexes **1** and **2** has prompted us to investigate the photoinduced insertion of CO_2 into the metal-hydrogen bond of **3a**. Photolysis of **1** and **2** under CO_2 in acetone or acetonitrile gave equimolar amounts of the formato complex *trans*-$[PtH(HCO_2)(PEt_3)_2]$ (**8**) and the solvento complex **4**, *trans*-$[PtH(S)(PEt_3)_2]^+$, with no evolution of H_2. The insertion reaction of CO_2 into the Pt-H bond does not occur thermally, and the monodentate formato complex **8** must be formed by the scavenging of the intermediate **3a** and by CO_2.

The results presented demonstrate that the solvent or purge with CO_2 exerts great control over the binuclear-forming reactions illustrated in Scheme III. Irradiation in acetonitrile or in chlorocarbon solvents as well as under CO_2 thus supresses the recombination between $[PtH_2(PEt_3)_2]$ and *trans*-$[PtH(S)(PEt_3)_2]^+$ and allows the reactions presented in sections 2-4 to be observed.

The electronic spectra of the trihydrido binuclear complexes **1** and **2** are listed in Table II. Calculations by Dedieu et al.[16] indicate that the LUMO energy level in complexes of this type has a metal-metal character, while the HOMO has antibonding metal d-orbital character. The irradiation using 335-nm light is expected to lead to the HOMO-LUMO transition (λ_{max} = 340 nm). Thus the primary excitation of **1** and **2** leads not only to a significant weakening of the Pt-Pt interaction but also to a cleavage of the $Pt_2(\mu\text{-}H)$ and $Pt_2(\mu\text{-}H)_2$ bridges. The wavelength dependence of the quantum yields (Table IV) substantiates the conclusion that HOMO-LUMO excitation is responsible for the photochemistry.

Experimental Section

FT-IR spectra were recorded with a Bruker IFS 88 spectrophotometer, UV-visible spectra with a Jasco-Uvidec 650 spectrophotometer, and NMR spectra with a Bruker 300 spectrometer. Chemical shifts are quoted with respect to Me_4Si. Analysis for H_2 by gas chromatography was carried out by using a Perkin-Elmer F17 gas chromatograph with a 5 Å molecular sieve column.

Both $[(PEt_3)_2HPt(\mu\text{-}H)PtH(PEt_3)_2][BPh_4]$ and $[(PEt_3)_2HPt(\mu\text{-}H)_2Pt(PEt_3)_2][BPh_4]$ were prepared and purified in accordance with the literature procedures.[5] All solvents used were purified and degassed. All described chemical manipulations were carried out under an inert atmosphere of argon.

Irradiation. Irradiations were carried out with an Applied Photophysics xenon lamp equipped with an *f*/3.4 monochromator. Light flux was measured by ferrioxalate actinometry.[14] The progress of the photoreactions was monitored by UV-visible spectral measurements. For the quantum yield determinations, the conversions to products were kept below 10%, and over this period, plots of conversion vs time were linear.

Photolysis of 1 or 2 in the Presence of PEt_3. A solution of complex **1** or **2** (0.15 mm) and PEt_3 (0.30 mm) in acetone was irradiated for 4 h at $\lambda \geq 335$ nm. During the irradiation a yellow precipitate formed. The precipitate was collected and identified by its ^1H NMR and IR spectra (Table I and III) as *trans*-$[PtH(PEt_3)_3][BPh_4]$.

Photolysis of Complexes 1 or 2 in Acetonitrile. Complex **1** or **2** (0.1 M) in acetonitrile was irradiated for 4 h. Analysis of the gases above the irradiated solutions showed the presence of H_2 (see GC Measurements). The solvent was removed in vacuo and the brown residue identified as a mixture of $[Pt(PEt_3)_3]$ and $[PtH(PEt_3)_3][BPh_4]$.

GC Measurements. A 10^{-3} M solution of **1** or **2** in CH_3CN was deoxygenated by bubbling with argon for 30 min. Photolyses of these solutions were carried out to completion (~4 h) by using 334-nm light. A sample of the gas phase above the irradiated solutions was extracted with a gas syringe and analyzed by GC (after a preliminary calibration had been made). The total H_2 evolved was $(0.5 \pm 0.1) \times 10^{-3}$ mol. GC analysis of the gases above a solution of 10^{-3} M **1** in $CHCl_3$ irradiated with ≥335-nm light for 4 h showed only C_6H_6; no H_2 was detected.

Radical-Trapping Experiments. Solutions of **1** or **2** (10^{-3} M) in carefully purified $CHCl_3$ were introduced into a 4-mm cylindrical ESR tube in the dark and degassed by bubbling with a slow stream of argon for 20 min. They were then introduced into the cavity of a Bruker ER 200 spectrometer. Irradiation was carried out with a Bruker lamp. The light ($\lambda > 330$ nm) was focused directly into the ESR cavity. The spin trap used was phenyl-*tert*-butylnitrone (PBN) in a 2×10^{-3} M concentration. The degassed solutions prepared in the dark did not show any signals. Upon irradiation (1 h) a signal consisting of a triplet of doublets is observed, which can be assigned to the $PhCH(CHCl_2)N(\dot{O})CMe_3$ adduct,[9] implying the formation of the radical $^{\bullet}CHCl_2$.

Acknowledgment. We thank Mr. S. Chaloupka for the preparation of the hydrido-bridged complexes used in this study. This work was supported by the Consiglio Nazionale Delle Ricerche (Progetto Finalizzato Chimica Fine).

Registry No. **1**, 84624-72-6; **2**, 81800-05-7; **3a**, 62945-61-3; **3b**, 80581-70-0; **4a**, 129364-91-6; **4b**, 129364-90-5; **5**, 22276-37-5; **6**, 39045-37-9; **7**, 16842-17-4; **8**, 81768-78-7; $CHCl_3$, 67-66-3; MeCN, 75-05-8; H_2, 1333-74-0; CO_2, 124-38-9.

(16) Dedieu, A.; Albright, T. A.; Hoffmann, R. *J. Am. Chem. Soc.* **1979**, *101*, 3141.
(17) Hatchard, C. G.; Parker, C. A. *Proc. R. Soc. London, Ser. A* **1956**, *235*, 518.

Contribution from the Department of Chemistry, Memorial University of Newfoundland, St. John's, Newfoundland, Canada A1B 3X7, and Division of Chemistry, National Research Council of Canada, Ottawa, Ontario, Canada K1A 0R9

Thiophenophane-Metal Complexes. 4. Structural and NMR Study of a 1,4-Fluxional Pivot about a Pd-S(thiophene) Bond

Shuang Liu,[†] C. Robert Lucas,*[,†] Michael J. Newlands,[†] and Jean-Pierre Charland[‡]

Received February 27, 1990

The preparation and X-ray structure of $[Pd(\eta^3\text{-allyl})(L)][CF_3SO_3]$ (L = $C_{10}H_{14}S_4$, 2,5,8-trithia[9](2,5)thiophenophane) are described. Crystal data for the complex: orthorhombic, space group $P2_12_12_1$; a = 8.7067 (4), b = 9.1259 (3), c = 22.540 (10) Å; Z = 4; R_F = 0.048, R_w = 0.050. The cation is pseudo-square-pyramidal with an exceptionally short apical Pd(II)-S(thiophene) bond length of 2.786 (4) Å. Effects of temperature and solvent on the NMR spectra of the complex are discussed. Observed spectral characteristics are explained by assuming the operation in solution of two processes. One is a 1,4-fluxional shift of $[Pd(allyl)]^+$ proceeding by a pivot about the Pd-S(thiophene) bond, while the other is a solvent-assisted dissociative inversion of thioether sulfur.

Introduction

We have been interested in the influence of structural constraints in macrocyclic thioether ligands upon the properties of their metal complexes and have reported recently several consequences of ligand rigidity.[1-3] In particular, we have described several Pd(II) and Pt(II) complexes of 2,5,8-trithia[9](2,5)thiophenophane, L, the solution NMR spectra of which are invariant with temperature and reflect clearly the highly rigid nature of

*Corresponding author.
[†]Memorial University of Newfoundland.
[‡]NRCC.

(1) Lucas, C. R.; Liu, S.; Thompson, L. K. *Inorg. Chem.* **1990**, *29*, 85.
(2) Lucas, C. R.; Liu, S.; Newlands, M. J.; Charland, J. P.; Gabe, E. J. *Can. J. Chem.* **1990**, *68*, 644.
(3) Lucas, C. R.; Liu, S.; Newlands, M. J.; Gabe, E. J. *Can. J. Chem.* **1990**, *68*, 1357.

0020-1669/90/1329-4380$02.50/0

Table I. Crystallographic Data for $[Pd(\eta^3\text{-}C_3H_5)(L)][CF_3SO_3]$

chem formula $C_{14}H_{19}F_3O_3PdS_5$	fw 559.02
a = 8.7067 (4) Å	space group $P2_12_12_1$
b = 9.1259 (3) Å	T = 22 °C
c = 22.5540 (10) Å	λ = 0.709 30 Å
ρ_{calcd} = 2.072 g cm^{-3}	μ = 16.2 cm^{-1}
V = 1792.06 Å^3	$R(F_o^2)$ = 4.8%
Z = 4	$R_w(F_o^2)$ = 5.0%

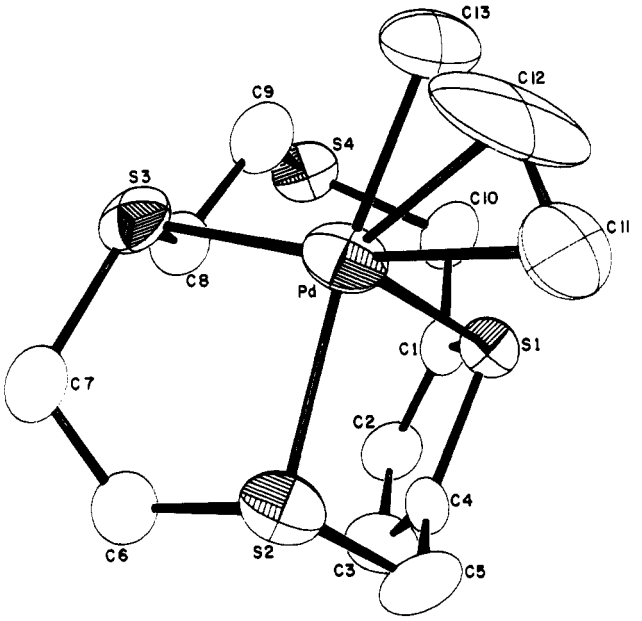

Figure 1. Molecular structure of the ion $[Pd(\eta^3\text{-}C_3H_5)(L)]^+$.

these complexes.[3] Their rigidity is, however, a consequence of several often subtle factors and not just structural constraints in the ligand, as the results reported herein will show. Rigidity and structural integrity or lack thereof in complexes of organic sulfur compounds are currently of considerable interest in several areas not the least of which involve studies of catalytic hydrodesulfurization[4] and of cellular sulfur donor reactions with platinum anticancer drugs.[5,6]

Experimental Section

Commercially available reagents were obtained from the Aldrich Chemical Co. Inc. or from Morton Thiokol Alfa Products Inc. and were used without further purification. We have previously described the preparation of ligand, L.[7] Spectroscopic data were obtained by using the following instruments: IR, Perkin-Elmer Model 283; NMR, General Electric 300-NB; UV/vis, Cary Model 17. X-ray data were collected by using an Enraf Nonius CAD-4 diffractometer. Analyses were performed by Canadian Microanalytical Services, Ltd.

Preparative Details. $[Pd(\eta^3\text{-}C_3H_5)(L)][CF_3SO_3]$. The dimer $[Pd(\eta^3\text{-}C_3H_5)Cl]_2$ (183 mg, 0.500 mmol) was dissolved in acetonitrile (15 mL), and $AgCF_3SO_3$ (257 mg, 1.00 mmol) in acetonitrile (5 mL) was added. The white precipitate that formed instantly was separated by filtration. A solution of 2,5,8-trithia[9](2,5)thiophenophane, L, (262 mg, 1.00 mmol) in CH_2Cl_2 (5 mL) was added to the filtrate. A small amount of precipitate was removed, and the resulting clear filtrate was left to evaporate slowly until yellow crystals were deposited. These were separated, washed with small amounts of acetone and then diethyl ether, and dried in air: yield 374 mg (67%); mp 180–185 °C dec. Infrared (Nujol mull): 3050 (w), 1425 (s), 1405 (m), 1385 (m), 1260 (s, br), 1185 (m), 1145 (s), 1025 (s), 960 (w), 940 (w), 920 (w), 900 (vw), 878 (m), 868 (m), 828 (s), 765 (m), 755 (m), 740 (w), 720 (m), 708 (m), 685 (s), 668 (m), 633 (s), 600 (vw), 570 (s), 515 (s), 495 (m), 460 (vw), 405 (w), 362 (w), 348 (w), 320 (vw), 298 (w), 272 (vw) cm^{-1}. Anal. Calcd for $C_{14}H_{19}F_3O_3PdS_5$: C, 30.08; H, 3.42; Pd, 19.03. Found: C, 29.92; H, 3.37; Pd, 18.70.

Table II. Positional and Thermal Parameters and Equivalent Isotropic Temperature Factors for $[Pd(\eta^3\text{-}C_3H_5)(L)][CF_3SO_3]$

atom	x	y	z	B_{iso}[a]
Pd	0.01667 (12)	0.24588 (12)	0.57519 (4)	3.68 (5)
S1	−0.0732 (4)	0.1458 (4)	0.68663 (16)	2.99 (14)
S2	0.2467 (4)	0.3040 (4)	0.61918 (16)	3.66 (15)
S3	−0.0716 (4)	0.4865 (4)	0.58768 (14)	3.62 (16)
S4	−0.4118 (4)	0.4078 (5)	0.71235 (16)	3.71 (16)
S5	0.4838 (6)	0.3800 (5)	0.87595 (17)	4.73 (19)
F1	0.512 (3)	0.1731 (17)	0.9413 (6)	13.8 (13)
F2	0.545 (4)	0.383 (3)	0.9726 (6)	22.5 (23)
F3	0.3285 (20)	0.3055 (21)	0.9589 (7)	12.9 (11)
O1	0.6461 (15)	0.3696 (17)	0.8679 (6)	6.7 (7)
O2	0.436 (3)	0.5228 (18)	0.8792 (7)	11.9 (12)
O3	0.391 (3)	0.293 (3)	0.8481 (8)	15.2 (16)
C1	−0.1740 (14)	0.2236 (15)	0.7385 (6)	2.9 (6)
C2	−0.0754 (17)	0.2918 (16)	0.7715 (6)	3.2 (6)
C3	0.0818 (18)	0.2817 (20)	0.7549 (7)	4.2 (7)
C4	0.1018 (15)	0.2100 (12)	0.7097 (6)	2.5 (5)
C5	0.2439 (16)	0.1935 (16)	0.6799 (7)	3.7 (6)
C6	0.2095 (16)	0.4871 (18)	0.6427 (7)	3.4 (7)
C7	0.1123 (19)	0.5727 (17)	0.6053 (6)	4.2 (7)
C8	−0.1708 (15)	0.4946 (17)	0.6512 (6)	2.9 (6)
C9	−0.3230 (18)	0.4160 (17)	0.6471 (6)	3.8 (7)
C10	−0.3457 (15)	0.2299 (18)	0.7360 (6)	3.6 (6)
C11	0.063 (3)	0.0219 (22)	0.5523 (9)	7.9 (12)
C12	−0.049 (4)	0.073 (4)	0.5273 (15)	13.6 (24)
C13	−0.165 (3)	0.1560 (24)	0.5280 (8)	7.0 (11)
C14	0.470 (3)	0.3156 (25)	0.9420 (8)	6.4 (11)

[a] B_{iso} (Å^2) is the mean of the principal axes of the thermal ellipsoid.

Table III. Selected Bond Lengths and Angles in $[Pd(\eta^3\text{-}C_3H_5)(L)][CF_3SO_3]$

Distances (Å)			
Pd–S(1)	2.786 (4)	S(4)–C(9)	1.664 (14)
Pd–S(2)	2.297 (4)	S(4)–C(10)	1.803 (16)
Pd–S(3)	2.343 (4)	C(1)–C(2)	1.294 (20)
Pd–C(11)	2.147 (18)	C(1)–C(10)	1.498 (18)
Pd–C(12)	1.995 (22)	C(2)–C(3)	1.421 (21)
Pd–C(13)	2.079 (18)	C(3)–C(4)	1.225 (21)
S(1)–C(1)	1.626 (14)	C(4)–C(5)	1.416 (19)
S(1)–C(4)	1.713 (13)	C(6)–C(7)	1.428 (21)
S(2)–C(5)	1.700 (16)	C(8)–C(9)	1.509 (21)
S(2)–C(6)	1.784 (18)	C(11)–C(12)	1.22 (4)
S(3)–C(7)	1.828 (17)	C(12)–C(13)	1.26 (4)
S(3)–C(8)	1.674 (13)		

Angles (deg)			
S(2)–Pd–S(3)	91.02 (14)	S(4)–C(9)–C(8)	112.1 (11)
S(2)–Pd–C(11)	99.1 (7)	S(4)–C(10)–C(1)	111.3 (10)
S(2)–Pd–C(12)	131.8 (9)	S(1)–C(1)–C(2)	105.4 (10)
S(2)–Pd–C(13)	167.8 (7)	S(1)–C(1)–C(10)	121.8 (10)
S(3)–Pd–C(11)	169.4 (6)	C(2)–C(1)–C(10)	131.8 (13)
S(3)–Pd–C(12)	135.3 (10)	C(1)–C(2)–C(3)	117.2 (13)
S(3)–Pd–C(13)	100.4 (7)	C(2)–C(3)–C(4)	113.0 (14)
C(11)–Pd–C(12)	34.1 (12)	S(1)–C(4)–C(3)	108.0 (11)
C(11)–Pd–C(13)	69.2 (9)	S(1)–C(4)–C(5)	126.7 (10)
C(12)–Pd–C(13)	36.1 (12)	C(3)–C(4)–C(5)	125.2 (13)
C(1)–S(1)–C(4)	96.4 (7)	Pd–C(11)–C(12)	66.1 (14)
Pd–S(2)–C(5)	101.5 (5)	Pd–C(12)–C(11)	79.8 (14)
Pd–S(2)–C(6)	100.8 (5)	Pd–C(12)–C(13)	75.6 (14)
C(5)–S(2)–C(6)	108.2 (7)	C(11)–C(12)–C(13)	149 (3)
Pd–S(3)–C(7)	98.2 (5)	Pd–C(13)–C(12)	68.3 (13)
Pd–S(3)–C(8)	108.3 (6)	S(1)–Pd–S(2)	86.0 (2)
C(7)–S(3)–C(8)	104.3 (7)	S(1)–Pd–S(3)	96.1 (1)
C(9)–S(4)–C(10)	98.9 (7)	S(1)–Pd–C(11)	87.6 (2)
S(2)–C(5)–C(4)	109.3 (9)	S(1)–Pd–C(12)	98.6 (2)
S(2)–C(6)–C(7)	116.3 (12)	S(1)–Pd–C(13)	96.8 (2)
S(3)–C(7)–C(6)	114.4 (11)	Pd–S(1)–C(1)	131.1 (2)
S(3)–C(8)–C(9)	112.3 (10)	Pd–S(1)–C(4)	85.0 (2)

X-ray Studies. A summary of crystal data for $[Pd(\eta^3\text{-}C_3H_5)(L)][CF_3SO_3]$ is in Table I. The diffraction intensities were collected at 295 K by using the $\theta/2\theta$ scan technique with profile analysis[8] at a scan speed of 4°/min. Three standards were measured after every 100 reflections,

(4) Blake, A. J.; Holder, A. J.; Hyde, T. I.; Küppers, H. J.; Schröder, M.; Stötzel, S.; Wieghardt, K. *J. Chem. Soc., Chem. Commun.* **1989**, 1600.
(5) *Platinum and Other Metal Coordination Compounds in Cancer Chemotherapy*; Nicolini, M., Ed.; Martinus Nijhoff: Boston, MA, 1988.
(6) Umapathy, P. *Coord. Chem. Rev.* **1989**, *95*, 129.
(7) Lucas, C. R.; Liu, S.; Newlands, M. J.; Charland, J. P.; Gabe, E. J. *Can. J. Chem.* **1988**, *66*, 1506.
(8) Grant, D. F.; Gabe, E. J. *J. Appl. Crystallog.* **1978**, *11*, 114.

and no significant crystal decay was detected. The space group was determined by systematic absences. Unit cell parameters in Table I were determined by a least-squares refinement of the setting angles for 10 reflections ($35° \leq 2\theta \leq 45°$). Lorentz and polarization factors were applied, and corrections were made for absorption.

The structure was solved with MULTAN[9] plus a difference Fourier map and refined by full-matrix least squares with counting statistics weights. H-atom positions were calculated, but their parameters were not refined. All heavier atoms were refined anisotropically. All calculations were performed with the NRCVAX crystal structure programs.[10] Scattering factors were taken from the usual source.[11] The final atomic positional parameters, the equivalent isotropic temperature factors, and important bond lengths and angles are listed in Tables II and III. Figure 1 shows a view of the molecule and its atomic number scheme.

Results

A structural study of $[Pd(\eta^3\text{-allyl})(L)][CF_3SO_3]$ has been conducted by X-ray methods, the results of which are presented in Figure 1 and Tables I–III. This new compound's NMR spectra in various solvents and at several temperatures have also been obtained and are given in Figures 2 and 4 and in Tables IV–VI. These results will be introduced at appropriate places in the discussion that follows.

Discussion

The electronic spectrum (Nujol mull or acetonitrile solution) is relatively featureless except for a shoulder at 340 nm on the low-energy side of an absorbance curve, which begins to rise steeply in that region. This shoulder is probably due to a S → Pd LMCT, since we have observed the same band in complexes of the form $MX_2{\cdot}L$ (M = Pd, Pt; X = Cl, Br, I, SCN), where it shifts appropriately in energy as M and X are varied.[3] Metal–sulfur stretching frequencies for these compounds are expected in the region 320 ± 20 cm^{-1} [12] and are usually weak. Furthermore, there are ligand absorptions in the same region,[7] which make it difficult to correlate any specific bands with Pd–S vibrations. Bands observed at 1260 (s, br), 1145 (s), 1025 (s), 828 (s), 755 (m), 720 (m), 633 (s), 570 (s), and 515 (s) cm^{-1} are typical of $CF_3SO_3^-$.[2]

As seen in Figure 1, the structure of the cation involves an η^3-allyl group and a chelating pair of thioether sulfurs from the thiophenophane that together give planar coordination to Pd. In fact, the four atoms S2, S3, C11, and C13 all lie within 0.01 Å of a plane defined by themselves, while the Pd atom is 0.063 Å above that plane and C12, the middle carbon of the allyl group, lies 0.220 Å below the plane. In addition to the η^3-allyl and pair of thioether sulfurs there is coordination in an apical site by thiophene sulfur. The average deviation of the apex-to-base bond angles from the ideal value of 90° is 1.6°, and the maximum deviation is 6.8°. The apical Pd–S1 bond length of 2.786 (4) Å is significantly less than the corresponding distance of 3.1817 (3) Å in $PdBr_2{\cdot}L$,[3] 3.125 Å in $[Pd(non)_2]^{2+}$ (non = 1,4,7-trithiacyclononane),[13] or 3.273 Å in $[Pd[18]aneS6]^{2+}$ ([18]aneS6 = 1,4,7,10,13,16-hexathiacyclooctadecane)[14] and much less than the sum (3.40 Å)[15] of the van der Waals radii of Pd and S. The average basal Pd–S length of 2.320 Å is slightly longer than corresponding averages of 2.279 Å in $PdBr_2{\cdot}L$,[3] 2.266 Å in $[Pd(non)_2]^{2+}$,[13] and 2.309 Å in $[Pd[18]aneS_6]^{2+}$ [14] but is approximately 17% shorter than the apical bond length. Interestingly, the apical Pd–S length of 2.786 (4) Å in this compound is the shortest apical Pd(II)–S bond known at this time even though the apical S is from thiophene. This short bond arises from a combination of the geometrical requirements of the ligand, which force S1 close to a metal whenever S2 and S3 are also coordinated,[3,16] and steric interactions of the allylic hydrogens particularly on C13 with hydrogens on the macrocycle that encourage a conformation that tips S1 even closer to Pd than in the related compound $PdBr_2{\cdot}L$.[3] It has been proposed in conjunction with hydrodesulfurization studies that coordination of thiophene in this way may lead to loss of aromaticity, signaled by folding of the ring, which eases subsequent steps leading to C–S cleavage and desulfurization.[17,18] In our structure, the thiophene ring does not deviate significantly from planarity although some bond length and angle distortions compared to the free ligand[7] may be noted. Presumably, the Pd–thiophene interaction, although short, is not strong enough to cause loss of aromaticity in the thiophene ring.[17]

Table IV. ^1H NMR Spectral Data for $[Pd(\eta^3\text{-}C_3H_5)(L)][CF_3SO_3]$ in CD_3NO_2[a]

assgnt	25 °C	95 °C
H2, H3	7.04 (s)	7.03 (s)
H12	5.98 (sept)[b]	5.98 (sept)[b]
syn H11, H13	4.92 (d)[b]	4.92 (d)[b]
H5A, H5B, H10A, H10B	4.23 (s)	4.22 (s)
anti H11, H13	3.72 (d)[b]	3.72 (d)[b]
H8B, H7A	3.06 (m)	3.06 (m)
H9B, H6B	2.81 (m)	2.81 (m)
H9A, H6A	2.57 (m)	2.57 (m)
H8A, H7B	2.14 (m)	2.16 (m)

[a] δ in ppm from internal TMS. [b] J(H12–syn H11, H13) = 7.2 Hz; J(H12–anti H11, H13) = 12.9 Hz.

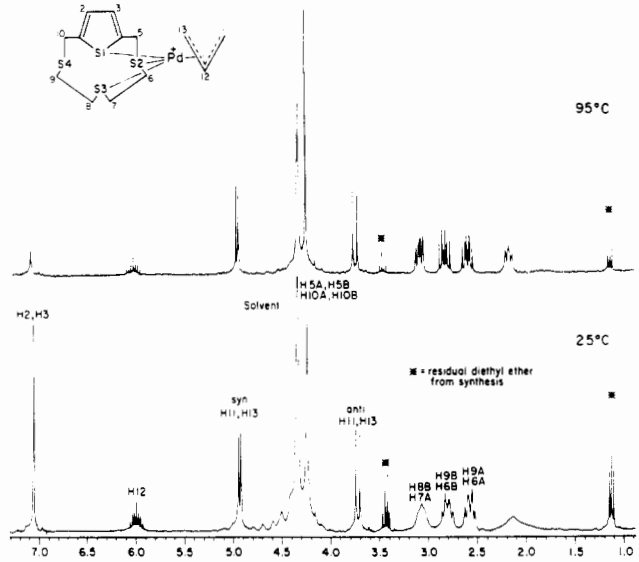

Figure 2. 300-MHz ^1H NMR spectra of $[Pd(\eta^3\text{-}C_3H_5)(L)][CF_3SO_3]$ in CD_3NO_2 (asterisk indicates residual diethyl ether).

The 300-MHz ^1H NMR spectra and spectral data of $[Pd(\eta^3\text{-}C_3H_5)(L)][CF_3SO_3]$ in CD_3NO_2 at 25 and 95 °C are in Figure 2 and Table IV. A striking feature is that the aromatic hydrogens, H2 and H3, give a singlet at 7.04 ppm from TMS instead of a pair of doublets as required by the solid-state structure and as observed[3] for structurally related $PdBr_2{\cdot}L$. The NMR equivalence of H2 and H3 is due to a 1,4-fluxional process that shifts the sites of ligand–metal attachment from S1, S2, and S3 to S1, S4, and S3. This process exchanges hydrogen sites in the aliphatic chain (Figure 3) in such a way that one hydrogen on C9 and one on C6 become equivalent as do the other hydrogens on C6 and C9 although the latter pair are never equivalent to the former pair. Likewise, one hydrogen on C8 and one on C7 become equivalent as do the other hydrogens on C8 and C7 although again the two pairs never become equivalent. Thus, signals from four distinct pairs of hydrogens are seen in the region 2–3 ppm from TMS.

(9) Germain, G.; Main, P.; Woolfson, M. M. *Acta Crystallogr., Sect. A* **1971**, *A27*, 368.
(10) Gabe, E. J.; Lee, F. L.; LePage, Y. In *Crystallographic Computing 3*; Sheldrick, G., Kruger, C., Goddard, R., Eds.; Clarendon Press: Oxford, England, 1985; p 167.
(11) *International Tables for X-ray Crystallography*; Kynoch Press: Birmingham, England, 1974; Vol. IV, Table 2.2B, p 99.
(12) Murray, S. G.; Hartley, F. R. *Chem. Rev.* **1981**, *81*, 365.
(13) Wieghardt, K.; Küppers, H. J.; Raabe, E.; Krüger, C. *Angew. Chem., Int. Ed. Engl.* **1986**, *25*, 1101.
(14) Blake, A. J.; Gould, R. O.; Lavery, A. J.; Schröder, M. *Angew. Chem., Int. Ed. Engl.* **1986**, *25*, 274.
(15) Bondi, A. *J. Phys. Chem.* **1964**, *68*, 441.
(16) Lucas, C. R.; Liu, S.; Newlands, M. J.; Charland, J. P.; Gabe, E. J. *Can. J. Chem.* **1989**, *67*, 639.
(17) Choi, M. G.; Angelici, R. J. *J. Am. Chem. Soc.* **1989**, *111*, 8753.
(18) Ogilvy, A. E.; Skaugset, A. E.; Rauchfuss, T. B. *Organometallics* **1989**, *8*, 2739.

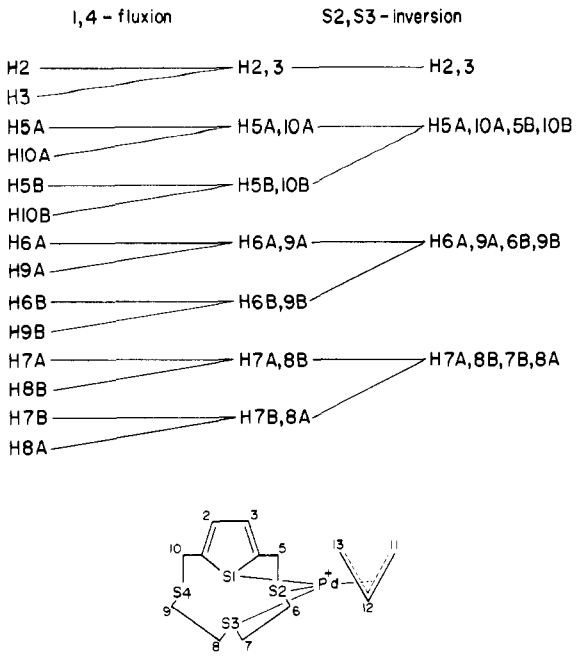

Figure 3. Site exchanges from stereochemical nonrigidity in $[Pd(\eta^3\text{-}C_3H_5)(L)]^+$.

The 1,4-fluxional process also interchanges C5 and C10 so that only one kind of thiophene-adjacent CH_2 is seen near 4.2 ppm from TMS. The fact that this signal is a broad singlet and not an AB quartet as expected is due to a solvent effect (vide infra). An alternative explanation for this singlet that is not based on a solvent effect but rather assumes inversions at the sulfurs is untenable. These inversions would also make the members of each pair of hydrogens on C6, C7, C8, and C9 equivalent (Figure 3) so that the combination of 1,4-fluxion and inversion would collapse this part of the spectrum to just two multiplets (C6, C9 hydrogens and C7, C8 hydrogens, as in the free ligand[7]) and not four as is observed.

It is apparent that a high-temperature-limiting spectrum for the 1,4-fluxional process has not been achieved at 25 °C because splitting in the multiplets at ~2.1 and ~3.1 ppm from TMS is unresolved at that temperature but becomes more clearly defined as the temperature is raised. Assignment of the multiplets (Table IV) to various exchanging sites is based on the fact that averages of the chemical shifts of corresponding hydrogens in rigid, nonfluxional $PdBr_2$·L accurately predict the multiplet positions in the spectrum of $[Pd(\eta^3\text{-}C_3H_5)(L)]^+$. These assignments are supported by the observation that those hydrogens in $PdBr_2$·L with the greatest chemical shift differences (H8A, H7B and H8B, H7A) are also those that require the highest temperatures to average their signals.

The spectrum of the $\eta^3\text{-}C_3H_5$ portion of the molecule is normal and can be viewed as that of an A_2B_2X system. It is invariant with temperature in the range 25–95 °C.

The 1,4-fluxional process can be detected in the ^{13}C NMR spectrum (Table V) also. There are only three signals from the hydrocarbon chain instead of six, as expected for a nonfluxional molecule. Furthermore, the terminal carbons of the allyl group are equivalent as are C1 and C4 in the thiophene ring. The signal for the exchanging C2 and C3 sites is at 118.35 ppm from TMS and is obscured by the broad signal from the CN carbon in the solvent except in an attached proton test spectrum. The CF_3 carbon in the anion is expected to have a very large coupling to fluorine, and as a result, its signal was not detected.

Fluxional processes involving heteroatoms are well documented[19-21] for 1,1-, 1,2-, or 1,3-shifts. Those involving 1,4-shifts are presently less well documented although examples are known,[22,23] one of which involves Pd(II) on secondary nitrogen. We believe, however, that the report herein is the first 1,4-fluxional process involving Pd(II) on thioether sulfur.

Table V. ^{13}C NMR Spectral Data for $[Pd(\eta^3\text{-}C_3H_5)(L)][CF_3SO_3]$ in CD_3CN[a]

assgnt	chem shift	assgnt	chem shift
C6, C9	30.52	C2, C3	118.35
C5, C10	34.32	C1, C4	121.39
C7, C8	36.03	C12	130.66
C11, C13	69.48		

[a] δ in ppm from internal TMS; spectra ^1H decoupled; assignments assisted by attached proton test.

The 1,4-fluxional behavior of $[Pd(\eta^3\text{-}C_3H_5)(L)]^+$ stands in sharp contrast to that of MX_2·L (M = Pd, Pt; X = Cl, Br, I, SCN), all of which are nonfluxional up to 140 °C.[3] Comparison of $PdBr_2$·L[3] and $[Pd(\eta^3\text{-}C_3H_5)(L)]^+$ reveals that in the allyl complex the Pd–S(thiophene) bond is 0.369 Å shorter, while the average basal Pd–S length is 0.041 Å longer. One could imagine, therefore, the short apical Pd–S bond in the allyl complex acting as a pivot around which the $[Pd(\eta^3\text{-}C_3H_5)]^+$ fragment could swing so that it coordinates to S2 and S3 at one time and to S4 and S3 at another. There will, of course, also be some minor conformational changes in the hydrocarbon chain that must accompany this pivot.

An alternative proposal that would involve thiophene sulfur in the apical position acting as an entering group in the normal substitution mechanism for planar d^8 metals seems unlikely, since it would involve a planar intermediate in which S1 and S3 are bonded to $[Pd(\eta^3\text{-}C_3H_5)]^+$. Furthermore, the complete 1,4-shift process would involve a 180° rotation of the $[Pd(\eta^3\text{-}C_3H_5)]^+$ fragment. This would require that all the allyl hydrogens be in changed environments and all allylic carbons be in unchanged environments after the 1,4-shift or else that C12 flip to keep H12 in the same orientation before and after the 1,4-shift and thereby exchange syn and anti hydrogens on both C11 and C13 while the C11 and C13 chemical shifts themselves are fortuitously the same. The ^1H NMR spectrum and its temperature dependence and the ^{13}C spectrum are inconsistent with these possibilities, and therefore, the pivot described earlier is the more plausible mechanism.

As already mentioned, the broad singlet in CD_3NO_2 solution spectra assigned to H10A, H10B, H5A, and H5B is not seen as an AB quartet due to solvent effects. This is demonstrated by the fact that the same signal in dimethyl-d_6 sulfoxide is a clearly resolved quartet at 30 °C with J_{AB} = 13.8 Hz. In deuterated *N*,*N*-dimethylformamide, the signal is also a quartet but $\Delta\delta$ is less and the outer pair of lines of the quartet have shrunk while the inner pair have grown in intensity. In deuterated acetonitrile, the value of $\Delta\delta$ is smaller still and the central pair of lines have coalesced to a very broad singlet and the outer pair are barely distinguishable from the base line, while in CD_3NO_2 the trend is continued except that residual CH_3NO_2 in the solvent produces a peak close enough to the H5A, H5B, H10A, H10B peak to obscure the weak outer lines of the AB quartet. We have also examined the spectrum of $PdBr_2$·L that we previously reported in DMSO-d_6[3] and which has a quartet for the signals from H5A and H5B. In acetonitrile-d_3, it too shows a decrease (~0.08 ppm) in $\Delta\delta$ for the H5A and H5B signals, which is sufficient for the central lines of the quartet to have almost coalesced. Not only does the solvent have an effect on the chemical shifts of the various signals but also it influences the types of processes occurring in the molecules. As a result, spectra of $[Pd(\eta^3\text{-}C_3H_5)(L)]^+$ in dimethyl-d_6 sulfoxide (Figure 4, Table VI) although similar to those in CD_3NO_2 differ in some respects. For example, the signal for H2 and H3 at 7.02 ppm from TMS is a singlet in DMSO-d_6 just as in CD_3NO_2 so the 1,4-fluxional process occurs in both

(19) Abel, E. W.; Bhargava, S. K.; Orrell, K. G. *Prog. Inorg. Chem.* **1984**, *32*, 1.
(20) Abel, E. W.; Orrell, K. G.; Quereshi, K. B.; Šik, V. *Polyhedron* **1988**, *7*, 1321.
(21) Abel, E. W.; Orrell, K. G.; Quereshi, K. B.; Šik, V. *Polyhedron* **1988**, *7*, 1329.
(22) Abel, E. W.; Beer, P. D.; Moss, I.; Orrell, K. G.; Šik, V.; Bates, P. A.; Hursthouse, M. B. *J. Chem. Soc., Chem. Commun.* **1987**, 978.
(23) Hunter, G.; McAuley, A.; Whitcombe, T. W. *Inorg. Chem.* **1988**, *27*, 2634.

Table VI. ^{1}H NMR Spectral Data for $[Pd(\eta^3\text{-}C_3H_5)(L)][CF_3SO_3]$ in DMSO-d_6[a]

assgnt	30 °C	60 °C	100 °C
H2, H3	7.02 (s)	7.01 (s)	7.00 (s)
H12	6.02 (sept)[b]	6.00 (sept)[d]	5.99 (quint)[e]
syn H11, H13	4.89 (d)[b]	4.89 (d)[d]	4.88 (br s)
H5A, H5B, H10A, H10B	4.33 (q)[c]	4.31 (q)[c]	4.23 (br s)
anti H11, H13	3.70 (d)[b]	3.72 (d)[d]	3.72 (br)
H8B, H7A	3.01 (br)	2.98 (br)	2.87 (br)
H9A, H6A, H9B, H6B	2.60 (br)	2.60 (br)	2.64 (br)
H8A, H7B	~2 (br)[f]	2.03 (br)	2.12 (br)

[a] δ in ppm from internal TMS. [b] J(H12–syn H11, H13) = 6.6 Hz; J(H12–anti H11, H13) = 12.8 Hz. [c] J_{AB} = 13.8 Hz. [d] J(H12–syn H11, H13) = 7.0 Hz; J(H12–anti H11, H13) = 12.9 Hz. [e] J(H12–H11A,B, H13A,B) = 10.0 Hz. [f] Averaging not complete; signal too broad to detect except by integration.

solvents and in neither is the high-temperature-limiting spectrum achieved at room temperature. In both solvents, the distinction between syn and anti types of terminal allylic hydrogens is retained at temperatures where the 1,4-fluxional motion is already fast. Therefore, the same intramolecular pivot is probably occurring in both solvents. In DMSO-d_6, the hydrogens on C5 and C10 appear as a well-resolved quartet at 40 °C whereas in CD_3NO_2 the signal appears to be a singlet (vide supra). The most striking differences between spectra in the two solvents, however, are in the region of ~2–3 ppm from TMS. Whereas the CD_3NO_2 solutions give well-resolved multiplets whose chemical shifts do not vary with temperature, in DMSO-d_6, the multiplets are unresolved broad bands that gradually merge into two broad bands as the temperature increases. These differences arise from reversible dissociation of L in DMSO-d_6 but not in CD_3NO_2. Although no signals due to free ligand are apparent in any of the spectra, indicating that the position of equilibrium in the dissociation lies far on the side of the complex, addition of small amounts of free ligand to the two solutions gives quite different results. In CD_3NO_2, sharp signals due to free ligand appear at the same chemical shifts as found for solutions of ligand only and these peaks do not change as the temperature is raised. In DMSO-d_6, however, the signals broaden and shift with increasing temperature until they merge with those of the complex. The relative integrated intensities in DMSO-d_6 of free and complexed ligand remain the same over the temperature range where they can be distinguished, thereby indicating that, at least to a first approximation, the degree of dissociation is not changing radically with temperature. Furthermore, DMSO-d_6 solutions with different concentrations of free ligand give signals that have the same width at half-height at corresponding temperatures, suggesting that concentration changes do not affect signal averaging or in other words that the processes are apparently unimolecular.

After dissociation, the free ligand may undergo inversions at S3 and S2 (or S4 since the S2, S4 distinction is lost on dissociation) so that upon recombination an enantiomeric form of the complex is produced. On any aliphatic carbon, the hydrogen that lies on the metal side of the macrocycle in one enantiomer becomes the hydrogen on the opposite side after the dissociation, inversions, and recombination. Thus, inversion plus the 1,4-fluxional process exchanges both hydrogens on C9 with both on C6 and both on C8 and C7 are likewise exchanged. As shown in Figure 3, this would lead to a high-temperature-limiting spectrum for the aliphatic portion of the molecule that would consist of a singlet and two multiplets. Unfortunately, at temperatures above 100 °C, signs of irreversible decomposition become apparent and the high-temperature-limiting spectrum was not observed.

Above 80 °C, the distinction between the syn and anti hydrogens in the allyl group begins to be lost, indicative of what is probably a conventional $\eta^3 \rightarrow \eta^1 \rightarrow \eta^3$ process.[24] Thus, the three processes have significantly different activation energies. The 1,4-fluxional process is already rapid on the NMR time scale at 40 °C, and although the dissociation/inversion process is also occurring at

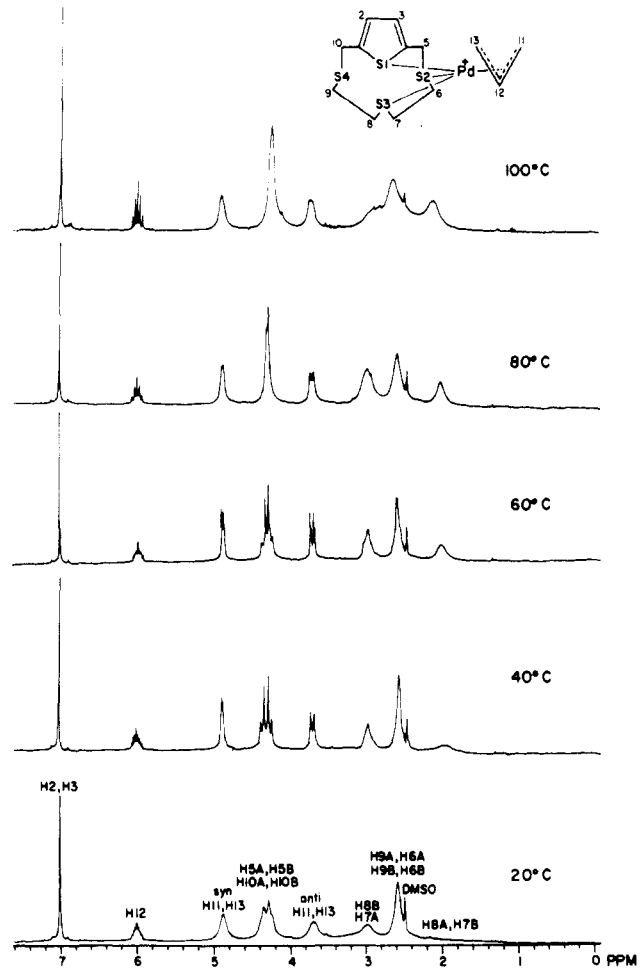

Figure 4. 300-MHz ^{1}H NMR spectra of $[Pd(\eta^3\text{-}C_3H_5)(L)][CF_3SO_3]$ in DMSO-d_6.

that temperature, it does not become rapid until approximately 90 °C. The allyl group's fluxional behavior is only beginning to become apparent at 80 °C, and even at 100 °C a syn/anti distinction between the terminal allylic hydrogens is still apparent. Although a high activation energy for the allyl fluxion is expected[25] and the activation energies for the S2, S3 inversion and 1,4-fluxion are expected to be lower, the relative energies of the latter processes are more difficult to predict. In general, 1,3-metal shifts occur at higher temperatures than do sulfur inversions although a recent report of these occurring at similar temperatures is also available.[20] None of these, however, may be truly comparable to the present situation where we are dealing with a 1,4-shift and with inversions in a sterically hindered system where dissociation apparently precedes inversion. Therefore, it is perhaps not so surprising that the effects of inversion are not seen in the NMR spectrum until the temperature is higher than that required to achieve the pivoting 1,4-shift.

Although an apparently unimolecular process, the role of solvent in the dissociation/inversion can be seen by comparing spectra in a variety of solvents. The results in *N*,*N*-dimethylformamide-d_7 are similar to those in DMSO-d_6, but in CD_3CN, the behavior is more like that in CD_3NO_2. Thus, in the strongly coordinating solvent DMSO-d_6, dissociation/inversion is more favored than in the more weakly coordinating solvent CD_3NO_2. This suggests that dissociation is assisted by coordination of solvent in the open octahedral site of the five-coordinate palladium atom in a manner analogous to that observed in general for solvent-assisted substitutions of planar, d^8 metal complexes.[26] Finally, it is consistent with this explanation that $PdBr_2$·L shows no solvent-assisted

(24) Faller, J. W.; Thompson, M. E.; Mattina, M. J. *J. Am. Chem. Soc.* **1971**, *93*, 2642.
(25) Cotton, F. A.; Faller, J. W.; Musco, A. *Inorg. Chem.* **1967**, *6*, 179.
(26) Atwood, J. D. *Inorganic and Organometallic Reaction Mechanisms*; Brooks/Cole: Monterey, CA, 1985; Chapter 2.

dissociation of its thioether-Pd bonds and that these bonds are on average 0.041 Å shorter than the corresponding bonds in $[Pd(\eta^3\text{-}C_3H_5)(L)]^+$, probably as a result of the differing trans effects of Br and allyl.

Acknowledgment. We thank the Natural Sciences and Engineering Research Council of Canada for financial support and Dr. P. D. Golding for helpful discussions.

Supplementary Material Available: Tables of anisotropic thermal parameters, hydrogen coordinates and thermal parameters, complete bond lengths and angles, and crystal data for $[Pd(\eta^3\text{-}C_3H_5)(L)[[CF_3SO_3]$ (4 pages); a listing of observed and calculated structure factors (9 pages). Ordering information is given on any current masthead page.

Contribution from the School of Chemical Sciences, University of Illinois, Urbana, Illinois 61801

Thiometalate Complexes Containing Arene, Thiophene, and Cyclobutadiene Coligands. Are Thiometalate Clusters Good Models for Desulfurization Catalysts?

Kevin E. Howard, John R. Lockemeyer, Mark A. Massa, Thomas B. Rauchfuss,* Scott R. Wilson, and Xiaoguang Yang

Received March 9, 1990

Reaction of $[(p\text{-cymene})RuCl_2]_2$ and $(PPh_4)_2WS_4$ gives $[(p\text{-cymene})RuCl]_2WS_4$; the corresponding $(C_6Me_6)Ru$ and (*p*-cymene)Os derivatives were also prepared. ^1H NMR and IR data suggest that these compounds comprise pairs of pseudooctahedral metal centers bridged by the tetrahedral WS_4. Related syntheses gave RuRe and Ru_2PtW_2 compounds from ReS_4^- and $Pt(WS_4)_2^{2-}$, respectively. The reaction of $(p\text{-cymene})RuCl_2(PPh_3)$ and $(PPh_4)_2WS_4$ gave $(p\text{-cymene})RuWS_4(PPh_3)$, whose structure was verified by X-ray crystallography. $(p\text{-cymene})RuWS_4(PPh_3)$ crystallizes in the monoclinic space group $P2_1/c$ (No. 14) with $a = 9.254$ (3) Å, $b = 15.690$ (8) Å, $c = 20.102$ (9) Å, $\beta = 98.77$ (3)°, and $Z = 4$. The analogous reaction of (tetramethylthiophene)-$RuCl_2(PPh_3)$ and $(PPh_4)_2WS_4$ results in the release of free tetramethylthiophene. In contrast, the *p*-cymene ligands were only labilized by further treatment of $[(p\text{-cymene})RuCl]_2WS_4$ with WS_4^{2-}. $[(C_4Me_4)NiCl_2]_2$ and WS_4^{2-} give $[(C_4Me_4)NiCl]_2WS_4$ while $(C_4Me_4)NiWS_4(PMe_2Ph)$ was prepared from $(C_4Me_4)NiCl_2(PMe_2Ph)$. $(C_4Me_4)NiWS_4(PMe_2Ph)$ crystallizes in the monoclinic space group *Ia* (No. 9) with $a = 13.294$ (6) Å, $b = 25.519$ (11) Å, $c = 13.186$ (6) Å, $\beta = 97.44°$, and $Z = 8$. Treatment of $[(C_4Me_4)NiCl]_2WS_4$ with $(Me_3Si)_2S$ gives a polymeric sulfided material, which upon pyrolysis evolves tetramethylthiophene.

Introduction

Organometallic derivatives of the tetrathio- and tetraseleno-metalates are a relatively new class of compounds comprised of organometallic subunits ligated to chalcogenometalate anions.[1-3] These bi- and multimetallic compounds have a rich chemistry with regard to their structural diversity, substitution reactions, and electrochemistry. Certain organometallic thiometalates show promise as precursors to new ternary chalcogenides.[3] Our work on platinum metal thiometalates has provided complexes with a variety of π-acidic ligands including carbon monoxide, olefins, isocyanides, allyl, and cyclopentadienyl.[4] Related work by Coucouvanis, Müller, and co-workers has afforded heterometallic thiometalates containing nitrosyl coligands.[5,6]

The present work concerns the synthesis of organometallic thiometalates containing arene, thiophene, and cyclobutadiene substituents. This project was originally undertaken to prepare structural models for the chemisorption of arenes and thiophenes on metal sulfides since it is well-known that certain metal sulfides catalyze the hydrogenation of arenes and the hydrogenolysis of thiophenes.[7] We expected to obtain some molecular-level insights into these heterogeneous processes by examining the structures and behavior of molecular analogues. In our scheme, the catalytic substrate is first attached to a metal halide, and this organometallic halide is then metathesized with a thiometalate anion. The strategy is reliable since suitable organometallic halides are available and the coordination chemistry of thiometalate is well established. Thiometalates,[8] typified by WS_4^{2-}, have been shown to coordinate either as $2e^-$ bidentate terminal ligands or as $6e^-$ bridging ligands, e.g., $Pt(WS_4)(diene)$[9] and $[(diene)Rh]_2(\mu\text{-}WS_4)$,[1] respectively.

The original tenet of this modeling effort was that thiometalate complexes would simulate reactivity characteristic of heterogeneous hydrodesulfurization (hds) catalysts. Thus, the complexes contain three known components of an hds catalyst system, i.e., substrates, catalytically active metals, and sulfur. As we will demonstrate, this simple recipe is flawed because it underestimates the effect of M:S stoichiometry, a factor known to be crucial to the activity of heterogeneous catalysts.[10] The effect of M:S stoichiometry is illustrated by a recent surface science study which shows that heavy sulfiding leads to thiophene *synthesis*, not thiophene desulfurization.[11] These experiments find precedent in the old thiophene synthesis from acetylene[12] or butadiene[13] and FeS_2.

Results

Arene Thiometalates. We prepared ruthenium and osmium arene thiometalates following the synthetic protocols used for

(1) Howard, K. E.; Rauchfuss, T. B.; Rheingold, A. L. *J. Am. Chem. Soc.* **1986**, *108*, 297.
(2) Howard, K. E.; Rauchfuss, T. B.; Wilson, S. R. *Inorg. Chem.* **1988**, *27*, 1710.
(3) Howard, K. E.; Rauchfuss, T. B.; Wilson, S. R. *Inorg. Chem.* **1988**, *27*, 3561.
(4) Howard, K. E. Ph.D. Thesis, University of Illinois at Urbana-Champaign, 1988.
(5) Coucouvanis, D.; Simhon, E. D.; Stremple, P.; Baenziger, N. C. *Inorg. Chim. Acta* **1981**, *53*, L135.
(6) Klingelhöfer, P.; Müller, U. *Z. Anorg. Allg. Chem.* **1988**, *556*, 70.
(7) Weisser, O.; Landa, S. *Sulfide Catalysts, Their Properties and Applications*; Pergamon Press: Oxford, England, 1973. *Hydrotreating Catalysts*; Occelli, M. L., Anthony, R. G., Eds.; Elsevier: Amsterdam, 1989.
(8) Müller, A.; Diemann, E.; Jostes, R.; Bögge, H. *Angew. Chem., Int. Ed. Engl.* **1981**, *10*, 934.
(9) Siedle, A. R.; Hubbard, C. R.; Mighell, A. D.; Doherty, R. M.; Stewart, J. M. *Inorg. Chim. Acta* **1980**, *38*, 197.
(10) Gellman, A. J.; Bussell, M. E.; Somorjai, G. A. *J. Catal.* **1987**, *107*, 103.
(11) Gentile, T. M.; Tsai, C. T.; Walley, K. P.; Gellman, A. J. *Catal. Lett.* **1989**, *2*, 19.
(12) Steinkopf, W. *Die Chemie des Thiophene*; Steinkopf, T., Ed.; Verlag von Theodor Steinkopff: Dresden, Germany, 1941; pp 8-11.
(13) Preparation of thiophene from FeS_2 and butadienes: Steinkopf, W. *Justus Liebigs Ann. Chem.* **1914**, *403*, 11.

0020-1669/90/1329-4385$02.50/0